Riccardi, Chiara; Wang, Di; Wistuba, Michael P.; Walther, Axel

Effects of polyacrylonitrile fibres and high content of RAP on mechanical properties of asphalt mixtures in binder and base layers

Published in:
Road Materials and Pavement Design

DOI:
10.1080/14680629.2022.2117072

Published: 01/01/2023

Document Version
Publisher's PDF, also known as Version of record

Please cite the original version:
Riccardi, C., Wang, D., Wistuba, M. P., & Walther, A. (2023). Effects of polyacrylonitrile fibres and high content of RAP on mechanical properties of asphalt mixtures in binder and base layers. *Road Materials and Pavement Design*, *24*(9), 2133-2155. https://doi.org/10.1080/14680629.2022.2117072

Taylor & Francis
Taylor & Francis Group

Road Materials and Pavement Design

ISSN: (Print) (Online) Journal homepage: https://www.tandfonline.com/loi/trmp20

Effects of polyacrylonitrile fibres and high content of RAP on mechanical properties of asphalt mixtures in binder and base layers

Chiara Riccardi, Di Wang, Michael P. Wistuba & Axel Walther

To cite this article: Chiara Riccardi, Di Wang, Michael P. Wistuba & Axel Walther (2023) Effects of polyacrylonitrile fibres and high content of RAP on mechanical properties of asphalt mixtures in binder and base layers, Road Materials and Pavement Design, 24:9, 2133-2155, DOI: 10.1080/14680629.2022.2117072

To link to this article: https://doi.org/10.1080/14680629.2022.2117072

ROAD MATERIALS AND PAVEMENT DESIGN
2023, VOL. 24, NO. 9, 2133–2155
https://doi.org/10.1080/14680629.2022.2117072

Effects of polyacrylonitrile fibres and high content of RAP on mechanical properties of asphalt mixtures in binder and base layers

Chiara Riccardi [a*], Di Wang [b*], Michael P. Wistuba [c] and Axel Walther[d]

[a]Department of Civil and Industrial Engineering, University of Pisa, Pisa, Italy; [b]Department of Civil Engineering, Aalto University, Espoo, Finland; [c]Department of Civil Engineering – Braunschweig Pavement Engineering Centre (ISBS), Technische Universität Braunschweig, Braunschweig, Germany; [d]Faculty of Civil and Enviromental Engineering, Ostfalia University of Applied Sciences, Suderburg, Germany

ABSTRACT

In this present study, the effects of polyacrylonitrile fibres and high content (50%) of Reclaimed Asphalt Pavement (RAP) on the mechanical properties of asphalt mixtures in binder and base layers were studied. This is the first time that the effect of high RAP content on the mechanical properties of fibre reinforced asphalt mixtures (FRAM) was evaluated, while the low temperature performance was not usually conducted in previous studies. Results indicated that the addition of polyacrylonitrile fibres worsens the moisture susceptibility resistance, but improves the rutting, stiffness properties, fatigue performances, and cumulative fatigue damage of the mixtures with and without RAP. No significant effects on the low temperature cracking resistance were found when fibre was used, while a remarkable improvement in the crack propagation resistance properties was observed. Therefore, the use of polyacrylonitrile fibres improves in general the mechanical responses of the mixture, especially in the stiffness response.

ARTICLE HISTORY
Received 30 March 2022
Accepted 21 August 2022

KEYWORDS
Fibers reinforced asphalt mixture; polyacrylonitrile fibres; RAP; mechanical properties; 2S2P1D

1. Introduction

Asphalt mixture is the one of the most widely used paving materials for road pavements (Liu et al., 2020; EAPA, 2022). It is continuously exposed to traffic loads and different environmental conditions which affect the short and long-term performance of the pavement. In past decades, continuously increased traffic volume and the environmental climate change demands, induced the enhanced durability and performance properties requirements for asphalt pavements (Office et al., 2021).

Different technologies were conducted to overcome these issues such as the addition of different types of fibres to improve the overall and/or specific mechanical properties (Button & Hunter, 1984; Motlagh & Mirzaei, 2016; Slebi-Acevedo et al., 2021). Varies types of fibres, such as cellulose (Landi et al., 2020), aramid (Ho et al., 2016), steel (García et al., 2015; Leiva-Padilla et al., 2019; Nguyen et al., 2017), polyolefin (Smirnova et al., 2019), polypropylene (Kim et al., 2018; Klinsky et al., 2018), glass (Eskandarsefat et al., 2019), lignin and asbestos (Chen et al., 2009) among others, were attempted in the laboratory and in the field to reinforce the asphalt mixture. Results indicated that in general, the

CONTACT Di Wang di.1.wang@aalto.fi

*Formerly at Technical University of Braunschweig, Beethovenstraße 51b, 38106 Braunschweig, Germany

fibre addition improves the resistance to fatigue cracking and rutting, and it works as a crack barrier to prevent the cracking propagation, while the effects on low temperature performance are seen quite controversially. The results showed that fibres could improve low-temperature fracture performance, however, such improvement highly rely on the fibre types, and for some fibres, such as lignin fibres, the improved effects are not stable (Wu et al., 2018).

In the early-stage work of the FIBRA project, the effect of different fibre's types on Asphalt Concrete (AC) and Porous Asphalt (PA) were evaluated through a multi-criteria design analysis method (Slebi-Acevedo et al., 2019, 2021; Bueno & Poulikakos, 2020). Results indicated that polyacrylonitrile (PAN) fibres lead to better overall chemo-mechanical properties for AC mixtures. Several researchers (Chen & Xu, 2010; Slebi-Acevedo et al., 2019; Wang et al., 2018; Weise & Zeissler, 2016; Xu et al., 2010) conducted on PAN fibres showed their reinforcement effects and the great networking function, leading to better rutting and fatigue resistance, while for the low temperature properties, the results were limited and discussed controversially (Tasdemir & Agar, 2007; Wu et al., 2018; Zhong et al., 2011). Besides the conventional mechanical properties, the effect of climate and traffic loading on the long-term pavement's mechanical performance was also studied in this project. In the authors' previous work (Walther & Wistuba, 2012; Wistuba & Walther, 2013), a mechanistic pavement design method was developed based on the linear-elastic multi-layer theory. The cumulative damage parameter was used to evaluate the long-term performance of asphalt mixtures based on German climate and performance requirements. More information are explained in chapters 2.2.5 and 3.5.

Nowadays, the use of RAP is a common environmentally, economically, and resource-efficient practice (Aurangzeb et al., 2014; Office et al., 2021). Generally, across Europe, the allowable amount of RAP that can be used in asphalt binder layers is around 30%, since the performance of asphalt mixtures changed dramatically for higher content of RAP. A plenty of studies were conducted to investigate the effects of high percentage of RAP on the performances of asphalt mixtures, especially on cracking resistance. Several researchers (Zhang et al., 2019; Zhou et al., 2019 and Montañez et al., 2020) showed that the addition of a high amount of RAP could shorten the fatigue life of asphalt mixtures, increasing the cumulative rate of fatigue damage. The use of RAP also worsens the low-temperature property of asphalt mixtures, making the mixtures more prone to thermal cracking (Zaumanis & Mallick, 2015; Riccardi et al., 2017b; Asib et al., 2019; Pedraza et al., 2021). Other results from laboratory and field evaluations showed that with an increasing of RAP content, the stiffness of asphalt mixtures increased, while fracture energy decreased (Van Winkle et al., 2017). Moreover, the addition of high amount of RAP could also have negative impacts on the short- and long-term aging behaviours (Majidifard et al., 2019), and on the self-healing property. Hence, the effect of the high content of RAP on the mechanical properties of FRAM was considered in this project, which is the first time in an experimental study.

To compensate for the negative effects of RAP, rejuvenators and/or softer asphalt binders are commonly added to the asphalt mixture to recover the rheological properties of the aged binder contained in RAP. Various types of non-renewable fossil-based rejuvenators show the capability to recover both short- and long-term performance properties of aged binder (up to 100%) (Hugener et al., 2022; Zaumanis et al., 2014). However, the use of alternative sustainable materials, such as fibres, may bring additional environmental benefits. Using fibres in substitution of polymers could help saving high amount of greenhouse gas (GHG) emission, energy consumption during the production and construction of asphalt mixtures, and save the non- renewable fossil-based products. This can be attributed to the relatively low mixing temperature. In fact, the fibres can be added at ambient temperature directly to the mix by using the dry process technology. Furthermore, the longer service life of FRAM could ultimately lead to an extra CO_2 emissions reduction during the operation period (Stempihar et al., 2012). Additionally, results showed that incorporating fibres with RAP could effectively improve the tensile strength, rutting resistance, and moisture susceptibility of asphalt mixtures, in addition to enhancing the resistance to crack initiation and propagation (Fakhri & Hosseini, 2017; Park et al., 2020; Ziari et al., 2020). However, each type of fibre presents its own disadvantages, for example, cellulose fibres mainly have the function of absorbing and stabilising asphalt binders rather than enhancing the strength of asphalt mixtures (Li et al., 2020). Polymer fibres exhibit inferior durability and dispersibility in asphalt

Table 1. Binders' conventional properties.

Binder types	Penetration [dmm] [EN 1426, 2015]	Softening point [°C] [EN 1427, 2015]	PG [AASHTO M320, 2021]
50/70	58.0	48.2	70–22
PmB 40/100-65	64.2	75.0	76–28
35/50	35.0	56.6	82–16
RAP binder	18.6	65.0	82–22

Table 2. Asphalt mixture types.

Mixture	Binder type	Binder content [%]	Fibre content [%]	Void content [–]
B-Ref.	50/70	4.4	0	5.8
B-PmB	40/100-65	4.4	0	5.5
B-FRAM	50/70	4.4	0.15	5.0
B-Ref + RAP	50/70 + RAP	4.4	0	5.5
B-PmB + RAP	40/70-65 + RAP	4.4	0	5.2
B-FRAM + RAP	50/70 + RAP	4.4	0.15	4.3
T-Ref.	50/70	4	0	6.5
T-FRAM	35/50	4	0.15	6.3

mixtures (Slebi-Acevedo et al., 2019), glass fibre shows poor adhesion with asphalt binder due to its smooth texture (Mukhammadiyeva et al., 2016).

In this study, the effects of adding PAN fibres on the overall mechanical performances of different asphalt mixtures containing high RAP contents were experimentally studied and modeled. Moreover, the cumulative fatigue damage was also calculated and compared based on a German-based mechanistic pavement design method.

2. Materials and testing

2.1. Materials

Two conventional binders: a 50/70 and a 35/50 Pen Grade (EN 12591, 2015) and a polymer modified binder 40/100-65 (EN 14023, 2010) were used to produce a set of eight mixtures for binder (B) and base (T) layers. These binders were chosen according to the German specification (TL Asphalt-StB 07/13, 2013), which indicate the use of 50/70 and 40/100-65 for the binder layer mixtures subjected to normal or heavy traffic and the use of 35/50 and 50/70 for the base layer mixtures subjected to heavy traffic. The characteristics of the binders, including also the extracted binder (EN 12697-3, 2013) from the RAP source are summarised in Table 1.

Five asphalt mixtures (Table 2) were prepared with fresh materials only: three of them for binder layers (B) and two of them for base layers (T). Considering the asphalt mixtures for binder layers, two of them were produced without incorporating fibres. The reference mixture (*B-Ref*) was produced using a plain 50/70 binder, while for the other one a 40/100-65 Polymer modified binder was used, and it is identified as *B-PmB*. The third one was a Fibre Reinforced Asphalt Mixture (*B-FRAM*) composed of 50/70 and 0.15% of PAN fibre of total weight of the asphalt mixture. Regarding the asphalt mixtures for base layers, the reference mixture (*T-Ref*) was produced with a 50/70 plain binder, while for the FRAM mixture (*T-FRAM*) a 35/50 plain binder was used together with 0.15% of PAN fibres. Other three mixtures for binder layers were prepared replacing 50% of the total weight by recycled materials originating from RAP. These mixtures were identified as *B-Ref + RAP*, *B-PmB + RAP* and *B-FRAM + RAP*.

All mixtures summarised in Table 2 have the following common characteristics:

- Same gradation curve as reported in Figure 1(a,b), typically used for the German (TL Asphalt-StB 07/13, 2013) binder and base layers, respectively;

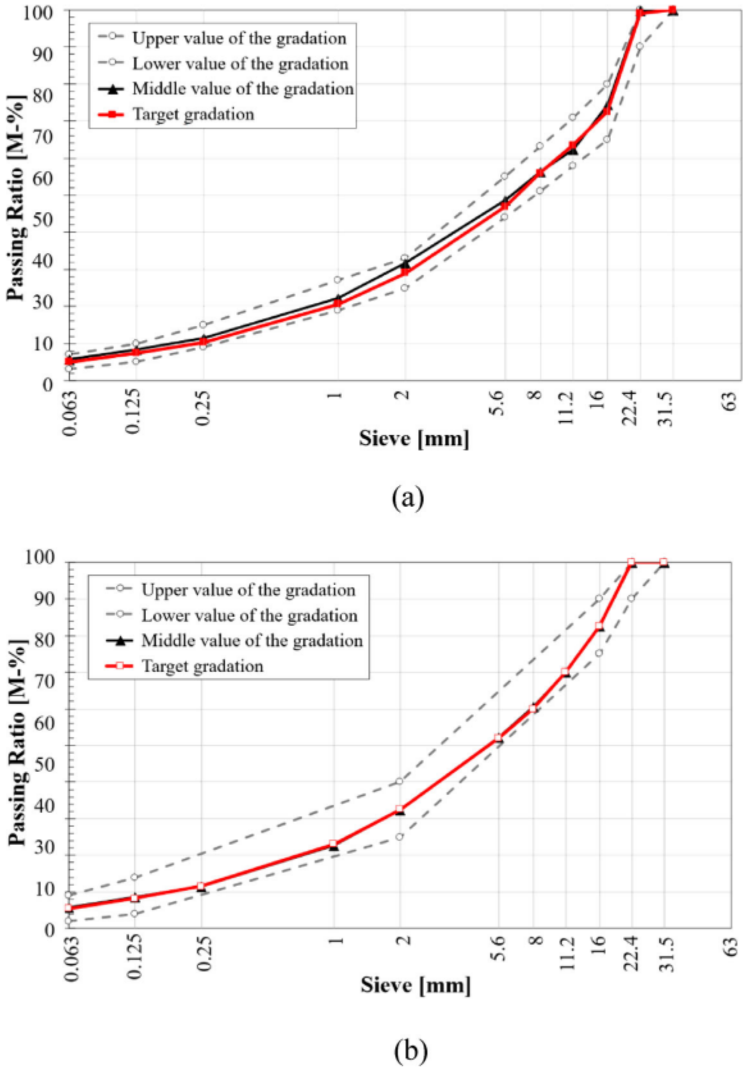

Figure 1. Standard grading curve (TL Asphalt-StB 07/13, 2013) used for asphalt mixtures for (a) binder layer and (b) base layer.

- Gabbro virgin aggregates and a single source of RAP material originating from a ten years' binder layer;
- 4.4% total binder content for the binder layer mixtures and 4% for the base layer mixtures by weight of the dry mix. The optimum binder content was chosen using the Marshall method (Roberts et al., 1991).
- Target air voids content: 5% for the binder layer mixtures and 6% for the base layer mixtures;
- Fibre content of 0.15% of the total weight of the asphalt mixture, added following the dry process, as suggested by the producer of the FRAM mixtures.

The physical and geometrical properties of the RAP source were also investigated. In particular, the black and white curves reported in Figure 2 were determined in accordance with EN 12697-2 (2013) and EN 13108-8 (2020). Then, the binder content of the RAP aggregates was determined on five samples with the rotatory evaporator (EN 12697-3, 2013) and resulted equal to 4.93%. The specific gravity was determined in accordance with EN 12697-5 (2019) and resulted 2.925 g/cm^3.

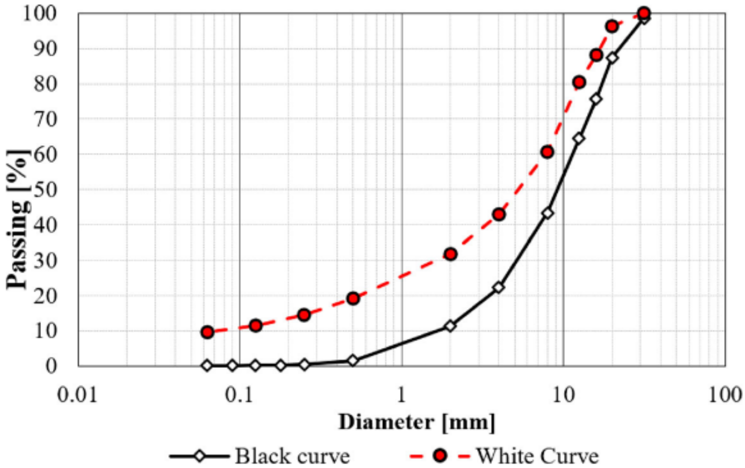

Figure 2. Black and White curves of the RAP source.

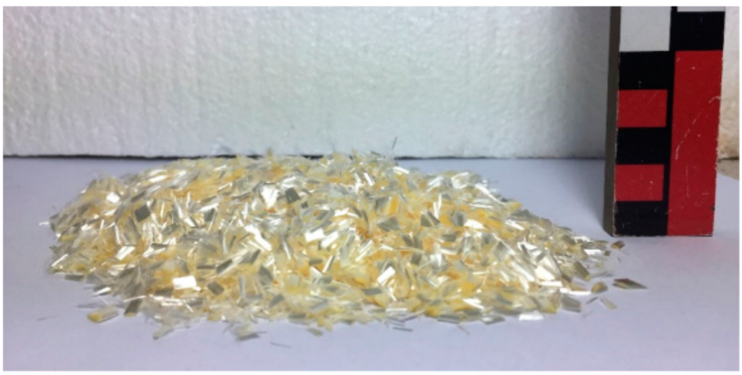

Figure 3. Illustration of PAN fibres.

PAN fibres (Figure 3) are synthetic, semi crystalline organic and thermoplastic fibres, its properties are summarised in Table 3. More information on thermal and chemical properties of these fibres, and of the microstructure of PAN incorporation within the mixtures can be accessed in FIBRA project's previous outcome (Bueno & Poulikakos, 2020).

From the slab of the mixtures compacted with the roller sector compactor (Wistuba, 2016), different samples were cut for carrying out the different tests. The detailed sizes are explained in the next chapter.

2.2. Mixture testing

To evaluate the mechanical properties of all the mixtures, different testing methods, described in the following, were carried out. The research approach adopted is summarised in Figure 4.

2.2.1. Water sensitivity test

A set of eight specimens ($D = 100$ mm, $h = 60$ mm) for each mixture was cored from slabs and was divided into two equally sized subsets and conditioned. One subset was maintained dry in a climate chamber at 22°C while the other subset was saturated and stored in water at elevated temperature (40°C) for 68–72 h. After conditioning, the indirect tensile strength of each of the two subsets was

Table 3. Characteristics of the PAN fibres.

Characterization	Description or parameters
Form	Staple fibres
Appearance	Bright straw yellow gold
Nominal diameter (μm)	10
Nominal length (mm)	4
Density (g/cm^3)	1.18
Humidity [%]	<2 or 18
Tenacity (MPa)	>708
Elastic modulus (MPa)	16,500
Elongation at break (%)	<13
Glass transition temperature T_g* in air [°C]	100
Melting temperature T_m* in air [°C]	330
Chemical resistance	All chemicals except Dimethylacetamide (DMAC); Dimethyl sulfoxide (DMSO); Dimethylformamide (DMF); $ZnCl_2$; Sodium thiocyanate (NaSCN)
Other resistance	Ultraviolet (UV), rot and weathering

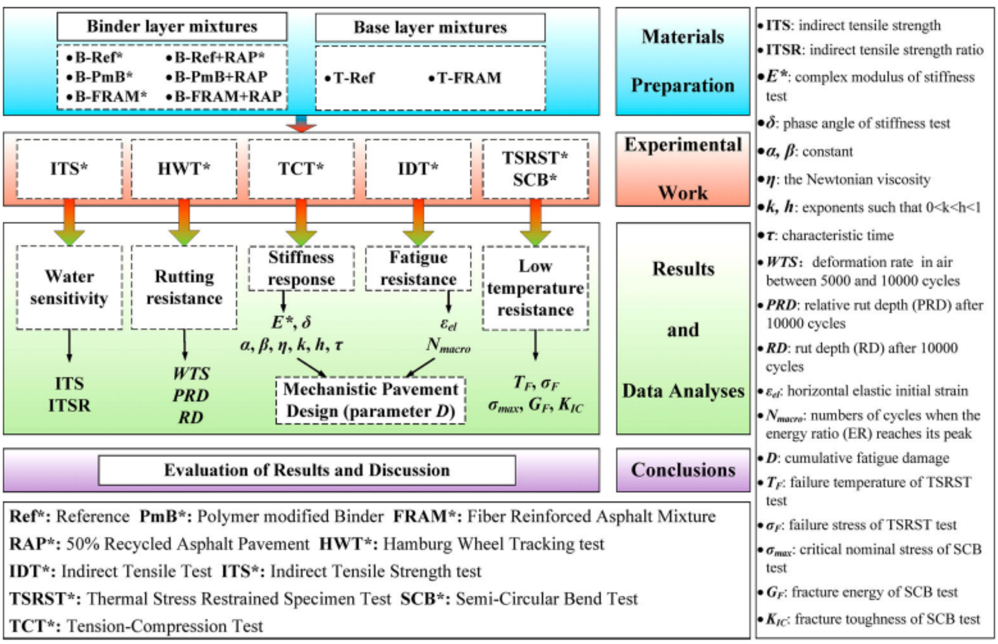

Figure 4. Research approach.

determined in accordance with EN 12697-23 (2017) at the specified test temperature of 22°C (Equation 1). The ratio of the indirect tensile strength of the water-conditioned subset compared to that of the dry subset was determined in accordance with Equation 2 and expressed in percentage (%) (EN 12697-12, 2018). The parameter of ITSR was applied to evaluate the effect of fibres.

$$ITS = \frac{2F}{\pi Dh} \tag{1}$$

$$ITSR = 100 \cdot \frac{ITS_w}{ITS_d} \tag{2}$$

Where ITS is the indirect tensile strength (MPa); F is the force (N); D and h are the diameter and the height in mm, respectively; $ITSR$ is the indirect tensile strength ratio, in percentage (%); ITS_w is the average indirect tensile strength of the wet group, and $ITS_d$is the average indirect tensile strength of the dry group.

2.2.2. Rutting resistance test

Hamburg Wheel Tracking (HWT) tests (EN 12697-22, 2020) were conducted to evaluate the rutting resistance. Compacted slabs (two replicators) with dimensions of 500 mm × 180 mm × 100 mm at a constant temperature of 60°C were used in this study. After a zero measurement the relative rut depth (*RD*), e. g., the absolute rut depth as a percentage of the specimen height (*PRD*), was determined at different time intervals together with a deformation rate *WTS* of between 5000 and 10000 cycles.

2.2.3. Stiffness test

Direct tension-compression tests in accordance with EN 12697-26 (2012) Annex D were performed on three replicates for each mixture type. According to the specification, a sinusoidal load was introduced into a cylindrical sample (50 mm × 160 mm) glued on two steel plates screwed to the loading rig. The stiffness tests were carried out at six different temperatures (−20, −10, 0, 10, 20 and 30°C) and six frequencies (0.1, 0.3, 1, 3, 5 and 10 Hz). In order to assure to be in the LVE range, a stress amplitude of 0.10 MPa was applied for temperatures from −20°C to 10°C, and 0.05 MPa was applied for 20 and 30°C. These stress amplitudes were chosen after conducting amplitude sweep tests at the lowest temperature and highest frequency, and at the highest temperature and lowest frequency, similar to what it's usually performed on the binder level (Riccardi, 2017).

The outputs are the stiffness modulus, E^*, and the phase angle, δ, versus frequency and temperature. The 2S2P1D model was used to fit the data (Di Benedetto et al., 2004; Olard & Di Benedetto, 2003; Possebon et al., 2021; Riccardi et al., 2017a and 2021; Nguyen et al., 2022). At reference temperature (10°C in this study), the 2S2P1D model expression for complex modulus is given by:

$$E^*(i\omega\tau) = E_0 + \frac{E_\infty - E_0}{1 + \alpha(i\omega\tau)^{-k} + (i\omega\tau)^{-h} + (i\omega\beta\tau)^{-1}} \tag{3}$$

where i is the complex number defined by $i^2 = -1$; ω is the angular frequency such that $\omega = 2\pi fr$ and fr is the reduced frequency; k and h are exponents such that $0 < k < h < 1$; α is a constant; E_0 is Young's modulus when $\omega \rightarrow 0$; E_∞ is the Young's modulus when $\omega \rightarrow \infty$; η is the Newtonian viscosity such that $\eta = (E_\infty\text{-}E_0)\beta\tau$; β is a constant; τ is the characteristic time, that governs the temperature dependency of the model and it represents the time needed for the system to relax. The characteristic time is function of temperature and based on the Time-Temperature Superposition Principle (TTSP) can be expressed as in Equation 4:

$$\tau(T) = a_T(T) \cdot \tau_0(T_S) \tag{4}$$

where a_T is the shift factor at temperature T; $\tau_0 = \tau(T_0)$ is the characteristic time determined at the reference temperature T_0. The shift factor at a specific temperature T, $a_t(T)$ can be obtained using Equation 5 (Williams et al., 1955).

$$\log a_T(T) = -\frac{c_1(T - T_0)}{c_2 + (T - T_0)} \tag{5}$$

Therefore, seven constants (E_0, E_∞, α, k, h, β and τ) are needed to entirely determine the linear viscoelastic behaviour of a specific asphalt mixture at a given temperature.

2.2.4. Fatigue resistance tests

To assess fatigue resistance of the mixtures, Indirect Tensile tests (IDT) (EN 12697-24, 2018) were carried out at a constant temperature of 20°C. Cylindrical specimens with dimensions of 100 × 40 mm² were cut from the slabs and were subjected to a continuous sinusoidal load in stress controlled mode at a frequency of 10 Hz. According to the standards, five loading amplitudes were used. The smallest

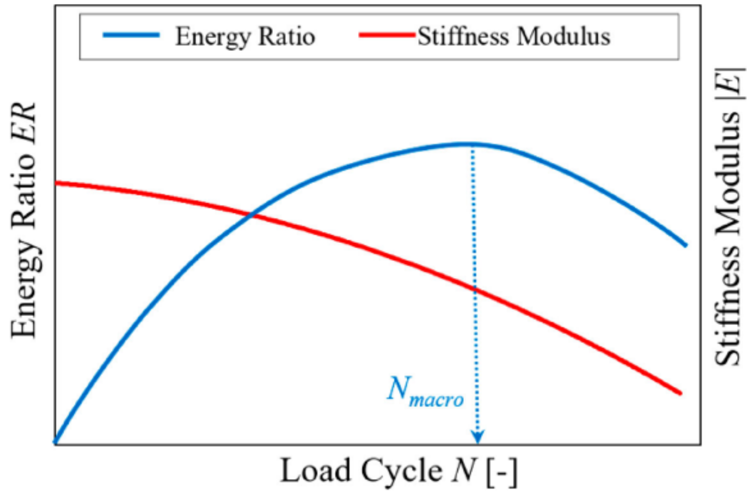

Figure 5. Schematic representation of N_{macro}.

loading amplitude was chosen in that way that the specimen fails after 10^6 cycles and the largest amplitude so that the specimen withstands at least 10^3 cycles. For each mixture, 15 specimens were tested (three samples for each of the five strain levels). The chosen fatigue failure criterion was based on the numbers of load cycles, N_{macro}, when the energy ratio (*ER*) (Figure 5) reaches its peak.

The *ER* is given by the product of the number of cycles and stiffness modulus (Equation 6):

$$ER(N) = |E(N)|N \tag{6}$$

Where *E(N)* is the stiffness modulus at the particular cycle *N*. The Wöhler line (Equation 7) (Saal & Pell, 1960) was used to express the material's fatigue law:

$$N_{Macro} = C_1 \cdot \varepsilon_{el}^{C_2} \tag{7}$$

Where ε_{el} is the horizontal elastic initial strain; C_1 and C_2 are fitting constants.

2.2.5. Mechanistic pavement design

The mechanistic pavement design was used in the present study to evaluate the fatigue evolution of the mixtures on site. This is based on an iterative design approach. The distress model is composed of individual sub-models displaying climate and traffic input data, distress analysis, and design decisions. The typical climate and traffic data in Germany were used in this study. For the distress model, the stiffness measured under 10 Hz at all six different temperatures, −20, −10, −0, 10, 20, and 30°C, were used as input data together with the fatigue parameters N_{Macro} and corresponding ε (EN 12697-24, 2018).

Analysis of fatigue evolution requires a cumulative damage hypothesis. This is realised by linear summation of cyclic ratios applying Miner's law (Miner, 1945; Monismith, 2004). The cumulative fatigue damage *D* due to load repetitions reads for a design period of 30 years can be expressed in:

$$D = \sum_{i=1}^{n} \frac{n_i}{N_{fi}} \leq 1 \tag{8}$$

Where, n_i is the number of actual traffic load application at strain/stress level *i*, and N_i is the number of allowable traffic load application to failure at strain/stress level *i*. Equation 8 allows predicting fatigue life in terms of the number of permissible load applications (due to traffic and thermal load cycles).

The mechanical analysis is based on a response model to calculate critical traffic-induced and/or temperature-induced stress. For this purpose, the pavement structure is represented by individual layers. In this study, a standardised asphalt pavement structure according to German regulations (AL Sp-Asphalt 09, 2009; RStO 12, 2012) is used exhibiting a thickness of 34 cm asphalt in total where 4 cm correspond to the surface layer (SMA), 8 cm to the binder layer and 22 cm to the base course. The binder and base layer, mixtures listed in Table 2 were used in this study. More detailed design approaches can be found in the authors' previous work (Wistuba & Walther, 2013).

2.2.6. Thermal cracking resistance and thermal fracture tests

2.2.6.1. Thermal stress restrained specimen test (TSRST). TSRST were performed in accordance with EN 12697-46 (2012) on prismatic asphalt beams with dimensions of $50 \times 50 \times 160\,\text{mm}^3$. During the test, the specimen was held at a constant length, while its temperature was decreased from a starting temperature of $+20$°C, with a constant cooling rate of $\Delta T = -10$ K/h. A close-loop control system kept the specimen at constant length. Due to the prohibited thermal shrinkage, the specimen was subjected to an increasing (cryogenic) tensile stress. The test ended at a minimum test temperature of $T = -40$°C or at failure, when the cryogenic stress reached the tensile strength of the asphalt sample. The TSRST results consisted in determining the failure stress σ_F and the failure temperature T_F.

2.2.6.2. Semi circular bending test (SCB). SCB fracture tests were performed based on EN 12697-44 (2019). Considering the climate conditions in Germany, a single test temperature of -18°C was selected in this study, at least two replications were performed for each mixture. More detailed information about the sample configuration and testing method can be found in the authors' previous studies (Cannone Falchetto et al., 2018). The critical nominal stress σ_{max}, and two main fracture parameters, fracture energy, G_F, and fracture toughness K_{Ic} were calculated by using the following equations:

$$G_F = W_F/A_{lig} = \int P du/A_{lig} \tag{8}$$

$$K_{Ic} = \sigma_{\max} \cdot Y_I \tag{9}$$

$$Y_I = -4.9965 + 155.58\left(\frac{a}{r}\right) - 799.94\left(\frac{a}{r}\right)^2 + 2141.9\left(\frac{a}{r}\right)^3 - 2709.1\left(\frac{a}{r}\right)^4 + 1398.6\left(\frac{a}{r}\right)^5 \tag{10}$$

Where W_F is the work of fracture; A_{lig} is the ligament area, given by $A_{lig} = (r\text{-}a) \times t$; Y_I is the normalised stress intensity factor (dimensionless); σ_{max} equals to $P_{max}/(2 \times r \times t)$; a is the notch length; r is the radius or the height of the sample and t is the sample thickness.

As shown in Equation 9, σ_{max} is the nominal stress recorded at the peak load, while K_{Ic} is the stress intensity factor at peak load, which represents the highest value of stress intensity factor that the material can bear before macro cracking occurs (when reached the peak load). Hence, both σ_{max} and K_{Ic} can be used to quantitatively evaluate asphalt mixtures' cracking resistance capability; in other words, these two parameters indicate the extreme thermal load that mixtures could endure. The value of G_F is the area under the load vs. load line displacement (LLD) curve by the ligament area (the product of the ligament length and the thickness of the specimen) of the SCB specimen prior to testing (EN 12697-44, 2019). Considering the curve shape, the value of G_F highly relies on the mixture's behaviour after peak load. A brittle material with a higher peak load and a sharp decreased curve may lead to a lower G_F, while softer material with a lower peak load and a gentle decreased line will ultimately result in a higher G_F. Such behaviour is mainly influenced by the interface between aggregates and binders (mastic). In a viscoelastic material such as asphalt mixture, the fracture energy increases with crack growth. Such increase is independent of crack length and growth speed, it only depends on the work needed for crack propagation. Therefore, a higher value of σ_{max} and K_{Ic} indicate a high strength

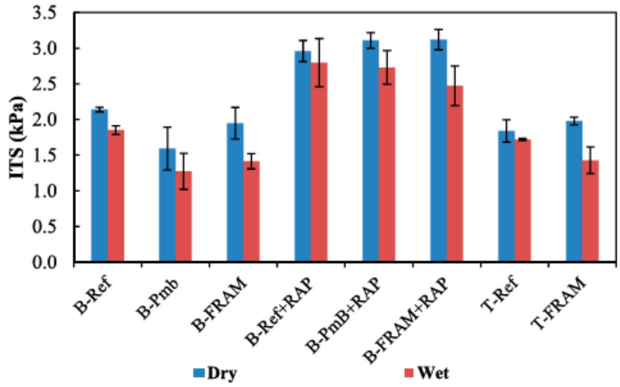

Figure 6. Indirect Tensile Strength results.

required to open the crack which means better resistance to thermal cracking before macro cracking occurs. In the meanwhile, a higher value of G_F indicates higher energy required for the crack to propagate which means a better resistance to crack propagation after macro-cracking.

3. Results and analysis

3.1. Water sensitivity results

Figure 6 presents the results concerning the ITS in both dry and wet conditions, including also the error bars to show the variability (standard deviation) of the measurements. It can be seen that the PmB and the mixtures containing RAP present higher variability of the measurements compared to the other mixtures. Moreover, the asphalt mixtures prepared with fibres result in similar or higher values of ITS in dry conditions compared to the polymer modified ones. In addition, it can be seen that the highest ITS values in both dry and wet conditions were found for the mixture composed of RAP. An increase between 27% and 48% for the dry condition, and 34% to 54% for the wet condition in comparison with the mixtures composed without RAP.

Concerning the moisture resistance of the mixtures, ITSR results are displayed in Figure 7. All the FRAM mixtures have shown lower moisture resistance compared to the reference and PmB mixtures. This can be due to the fact that the fibres may absorb the moisture, which may lead to binder stripping, causing failure at lower stress (Gupta et al., 2021). This would be consistent with the hypothesis that this type of fibre improves the mechanical performance of the mixture under dry conditions but requires a greater amount of binder to work properly also in wet condition. However, all the values of the ITSR were higher than 70% fulfilling the German specification for binder and base course.

3.2. Rutting tests results

Table 4 displays the results of the Hamburg wheel tracking tests (EN 12697-22, 2020). For each mixture, the deformation rate (*WTS*) between 5000 and 10000 cycles, the rut depth (*RD*) after 10000 cycles and the relative rut depth (*PRD*) after 10000 cycles were calculated.

According to these results, the mixtures containing fibres (*B-FRAM*, *B-FRAM + RAP*, *T-FRAM*) depicted remarkable improvements in all the parameters (*WTS, RD, PRD*) in comparison to the reference mixtures (*B-Ref*, *B-Ref + RAP*, *T-Ref*) and slightly worse performance than *B-PmB*. However, both mixtures *B-FRAM* and *B-PmB* present an excellent rutting resistance, largely respecting the standard requirements for binder layer mixtures which for the highest traffic category, impose a maximum slope of 0.070 mm/1000 cycles. Also with the incorporation of RAP, the fibres improve the permanent deformation resistance. Hence, it can be concluded that in the high temperature range, the addition of

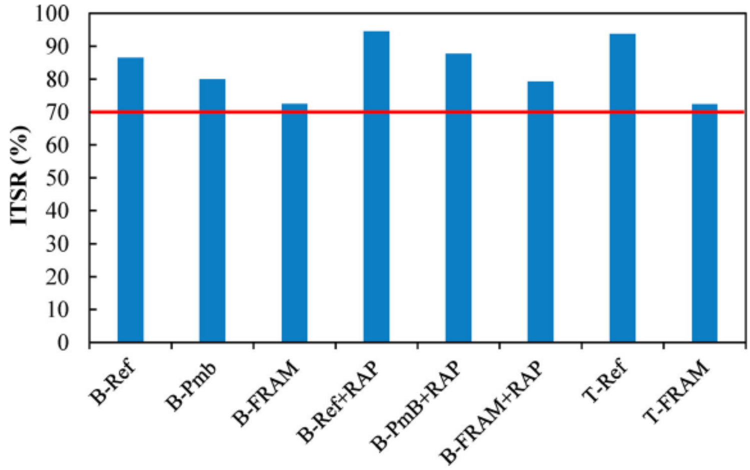

Figure 7. ITSR results on the different mixtures.

Table 4. Rutting test results.

Mixtures	*WTS* [mm/1000cycles]	*RD* [mm]	*PRD* [%]
B-Ref	0.030	2.32	3.6
B-PmB	0.016	1.42	3.2
B-FRAM	0.021	2.05	3.3
B-Ref + RAP	0.016	1.88	3.2
B-PmB + RAP	0.011	1.64	2.6
B-FRAM + RAP	0.013	1.58	2.5
T-Ref	0.036	2.89	4.4
T-FRAM	0.009	1.70	2.5

the fibres in the mixtures has a positive effect, acting as a reinforcement and improving the rutting resistance of the mixtures.

3.3. Stiffness tests results

Figure 8 reports the master curves of the complex modulus and of the phase angle for binder and base layers' mixtures at a reference temperature of 10°C fitted with the 2S2P1D model. For binder layer (Figures 8(a,b)), the reference mixture, *B-Ref*, composed with the 50/70 binder presents the highest complex moduli compared to the *B-PmB* and *B-FRAM* mixtures. In more details, it was found that the complex moduli of the *B-FRAM* mixture are always between the ones of the *B-Ref* and *B-PmB* mixtures. For the mixtures containing RAP, the stiffening effect of the aged binder present in RAP can be seen, which increases significantly the stiffness values up to more than the double of the mixtures without RAP. Similar results in terms of the complex moduli were found for the RAP mixtures. Looking at the phase angle, it can be seen that in the high frequencies/low temperature range, the *B-FRAM* mixture gives similar values to the *B-Ref* and *B-PmB*; while at low frequencies/high temperature, and at intermediate temperature, the phase angles of the *B-FRAM* are lower than the ones of the *B-PMB* mixture, indicating a less viscous behaviour; while the *B-Ref* mixture presents the highest phase angle and therefore a more viscous behaviour. For the mixtures containing RAP, the *FRAM + RAP* mixture presents the lowest phase angle especially in the low frequencies/high temperatures range in comparison with all the other mixtures indicating a more elastic behaviour in all the temperature ranges.

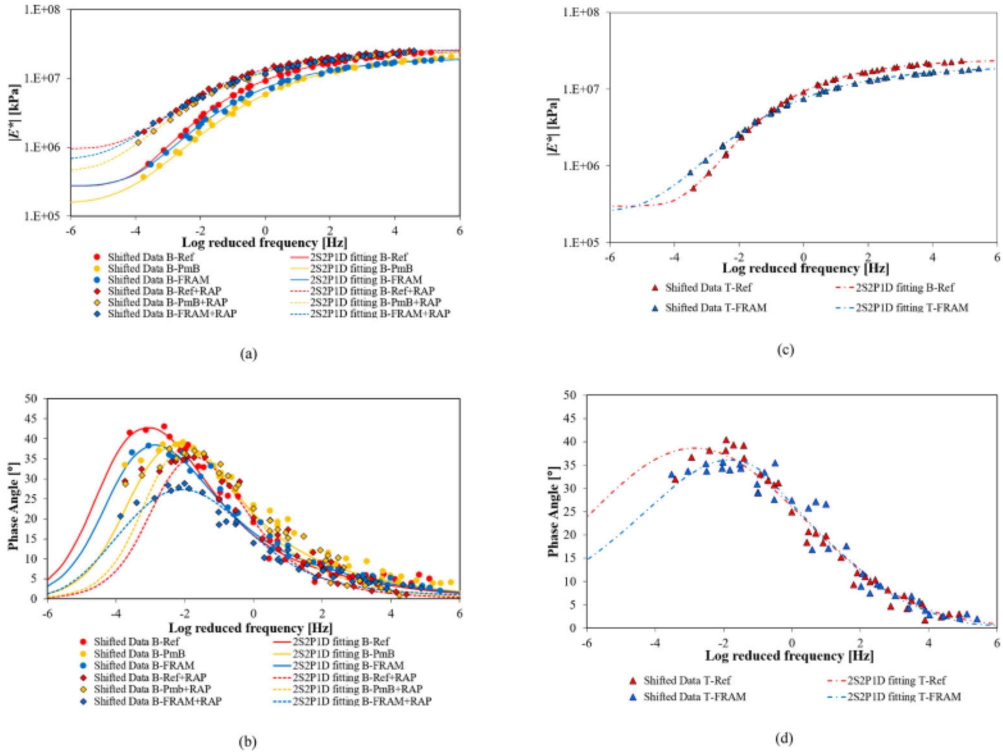

Figure 8. Master curves of the mixtures at a reference temperature of 10°C: (a) binder layer complex modulus $|E^*|$; (b) binder layer phase angle δ; (c) base layer complex modulus $|E^*|$; (d) base layer phase angle δ.

It can be concluded that the mechanical behaviour of the B-FRAM mixture is similar to or even better than the corresponding B-PmB mixtures in the LVE range. It is noting the mechanical property of FRAM (fibre and plain binder) is similar to or even better than the polymer-modified mixture. Regarding the addition of fibres in RAP mixtures, it seems to have a significant effect in the high-temperature range. Because the phase angles of the B-FRAM + RAP are the lowest which indicates that the fibres make the mixture less viscous.

As shown in Figure 8(c,d) for the base layers' mixtures, very similar results in terms of complex moduli and phase angles were obtained for *T-Ref* and *T-FRAM*. In more details, slightly lower complex moduli and higher phase angle were found for the *T-FRAM* mixture in the high frequency/low-temperature range, while higher complex moduli and lower phase angles were found in the low frequency/high-temperature range, indicating better mechanical properties in comparison to the *T-Ref* mixture. Therefore, it can be concluded that in the base layer mixture the addition of the fibres to the plain binder 35/50 make the mixtures more elastic and less stiff at low temperature, while they act as a reinforcement at high temperature making the mixtures stiffer and more viscous.

Figure 9 displays the Cole–Cole and black diagram fitted with the 2S2P1D model. The Cole–Cole plot expresses the relationship between the real (E') and imaginary (E'') components of the complex modulus (E^*), while the black diagram expresses the relationship between the complex modulus (E^*) and the phase angle (δ). From these plots it can be seen that *B-FRAM* has the lowest maximum values of E'' and of the phase angle indicating a smaller viscous tendency with respect to *B-Ref* and *B-PmB*. In particular, it can be observed that the *B-Ref* mixture reaches a maximal phase angle of 43°, that is 8° higher than the one of *B-FRAM* mixture which reaches a maximal phase angle of 35°, and 3° higher than the one of *B-PmB*, which presents a maximal phase angle of 40°C. All the parameters of the model together with the coefficients of the WLF equation are summarised in Table 5. The parameters of the

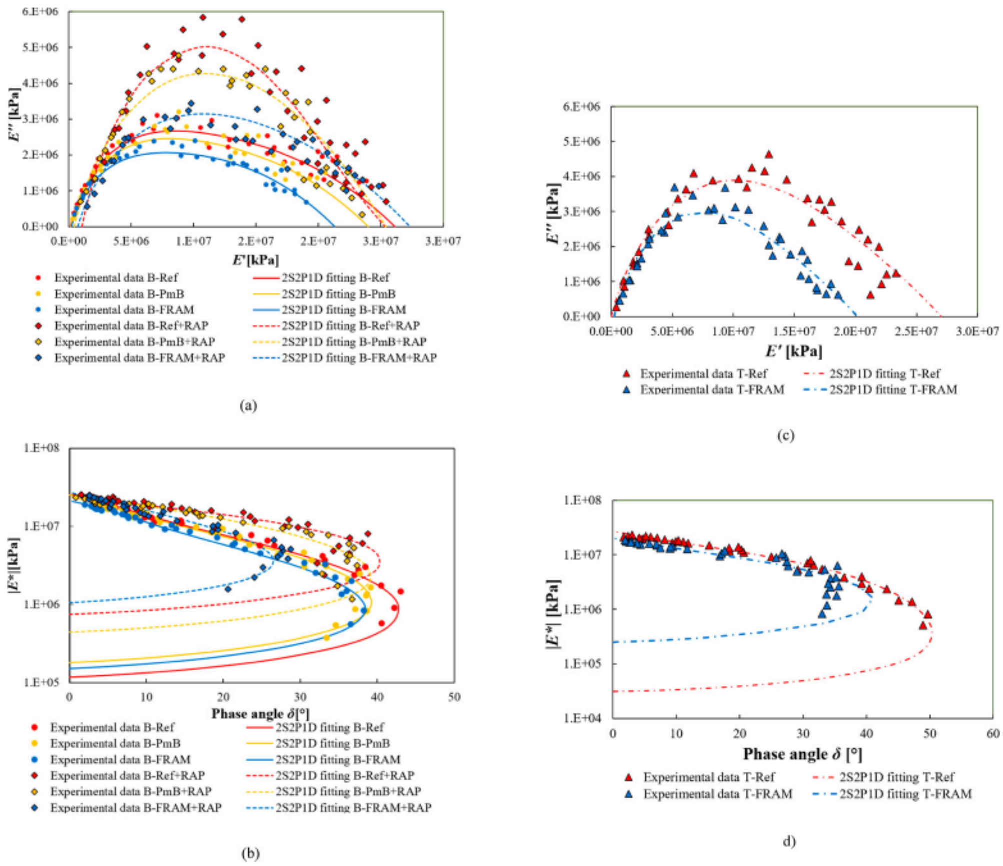

Figure 9. Experimental data and 2S2P1D fitting displayed in (a) binder layer Cole-Cole plot; (b) binder layer black-diagram; (c) base layer Cole-Cole plot; (d) base layer black-diagram.

2S2P1D model help to provide a better understanding of the effects of adding fibres in the mixture with and without RAP. It's well known that the parameters k, h, α and β are related to binder properties [38, 39, 48]. Comparing *B-Ref* and *B-FRAM*, it can be seen that the addition of fibres doesn't change these parameters significantly. This means that adding the fibres on the plain binder has no significant effects on binder rheology. Regarding *B-PmB*, lower values of the parameter α, which governs the height of the peak in the Cole–Cole plot, and of h, which governs the slope at high temperature, were found compared to the other two mixtures. Also the characteristic time, τ_0, was found to be lower for *B-FRAM* and *B-PmB* compared to *B-Ref*. This indicates a shorter relaxation time for the mixtures containing fibres and polymers. Regarding the other parameters, E_0 is the static modulus and is associated with the aggregate skeleton and void content (Nguyen et al., 2015) and E_∞ is the glassy modulus. It was found that *B-PmB* presents the highest value of E_0, similar to the *B-FRAM* and as latest the *B-Ref*, demonstrating the reinforcement effects of the fibres in the high temperature range. The *B-FRAM* mixture presents the lowest value of E_∞ showing the potential to have a less stiff material in the low temperature range.

For the base layer mixtures, *T-FRAM* presents lower values of E'' and of δ with respect to the *T-Ref* mixture, in accordance with the results of the binder layer mixture. All the parameters of the 2S2P1D model are higher than the ones of *T-Ref* showing the reinforcing effect of the fibres which give also a more elastic behaviour to the mixture.

Table 5. 2S2P1D model parameters.

Mixtures	E_0[kPa]	E_∞[kPa]	α	τ_0	k	h	β	c_1	c_2	R^2
B-Ref	1.18E+05	2.61E+07	2.56	0.99	0.21	0.63	449.9	177.9	1318	0.99
B-PmB	1.81E+05	2.40E+07	2.10	0.63	0.22	0.58	449.9	52.1	394.2	0.99
B-FRAM	1.51E+05	2.13E+07	2.50	0.86	0.21	0.62	449.9	48.5	355.2	0.99
B-Ref + RAP	7.52E+05	2.53E+07	1.10	0.55	0.28	0.65	499.9	54.7	456.9	0.99
B-PmB + RAP	4.43E+05	2.54E+07	1.80	0.50	0.28	0.68	450.0	56.7	419.8	0.99
B-FRAM + RAP	1.05E+06	2.73E+07	1.80	0.78	0.26	0.56	450.0	42.0	358.1	0.99
T-Ref	3.10E+04	2.50E+07	2.97	1.51	0.23	0.60	150.0	64.8	433.5	0.99
T-FRAM	2.50E+05	2.02E+07	4.07	3.92	0.26	0.67	149.9	51.5	374.	0.99

Table 6. Stress levels applied for the IDT tests to the different mixtures.

Mixtures	σ_0 [MPa]
B-Ref	0.15, 0.20, 0.25, 0.30, 0.35
B-PmB	0.20, 0.25, 0.30, 0.35, 0.40
B-FRAM	0.10, 0.15, 0.20, 0.25, 0.35
B-Ref + RAP	0.30, 0.35, 0.40, 0.45, 0.50
B-PmB + RAP	0.30, 0.40, 0.50, 0.60, 0.70
B-FRAM + RAP	0.35, 0.40, 0.50, 0.60, 0.70
T-Ref	0.50, 0.60, 0.70, 0.80, 0.90
T-FRAM	0.40, 0.50, 0.60, 0.70, 0.80

Focusing on the mixtures containing RAP, similar trends can be found in the Cole–Cole plot and in the black diagram. In fact, the *B-FRAM + RAP* mixture presents the lowest values of E'' and of δ in comparison with the other two mixtures containing RAP. In particular, it can be noticed that the *B-Ref + RAP* mixture has a maximal phase angle of 40°, which is 14° higher than the maximal value for *B-FRAM + RAP*. Regarding the parameters E_0 and E_∞, the *B-Ref + RAP* presents the highest values compared to the other two mixtures with RAP. This indicates a stiffer material both in the high and low temperatures range, but with a more elastic behaviour. Looking at the fitting parameters, the mixtures containing RAP present lower values of α and higher values of *k, h,* and τ_0 than the mixtures without RAP. This clearly shows the stiffening effects of the addition of the RAP in the mixture, which significantly changes the rheological behaviour of the base binder composing the mixture.

3.4. Fatigue tests results

Figure 10 displays the results of the IDT tests for all the mixtures according to EN 12697-24 (2018). Five different stress levels, summarised in Table 6, were used for each mixture. In Figure 10, the Wöhler curves are reported together with the fatigue laws based on the energy ratio (*ER*) described in chapter 3.2.4 for the binder and base layers respectively.

As shown in the previous figures, very good repeatability was found for all the mixtures (AL Sp-Asphalt 09, 2009), where for binder layers mixtures the R^2 should be greater than 0.90 and for base layer mixture should be higher than 0.80. It can be noticed that the *B-PmB* mixture presents the best fatigue performance in the strain range of the experiments, followed by *B-FRAM* and *B-Ref.*

B-FRAM has a lower slope of the fatigue line compared to *B-PmB*, indicating better fatigue performance under higher strain levels. In particular, *B-FRAM* has best fatigue performance under strains greater than 0.6‰, which is the value of the intersection between the two fatigue lines of *B-FRAM* and *B-PmB.*

Regarding the mixtures containing 50% of RAP, similar fatigue resistances for *B-Ref + RAP* and *B-FRAM + RAP* were found. These fatigue lines are almost parallel to the Wöhler curve of *B-PmB + RAP* which presents best fatigue resistance. Generally, it can be observed that the fatigue lines for the RAP mixtures are very close to one another indicating comparable fatigue performances. Moreover, it can

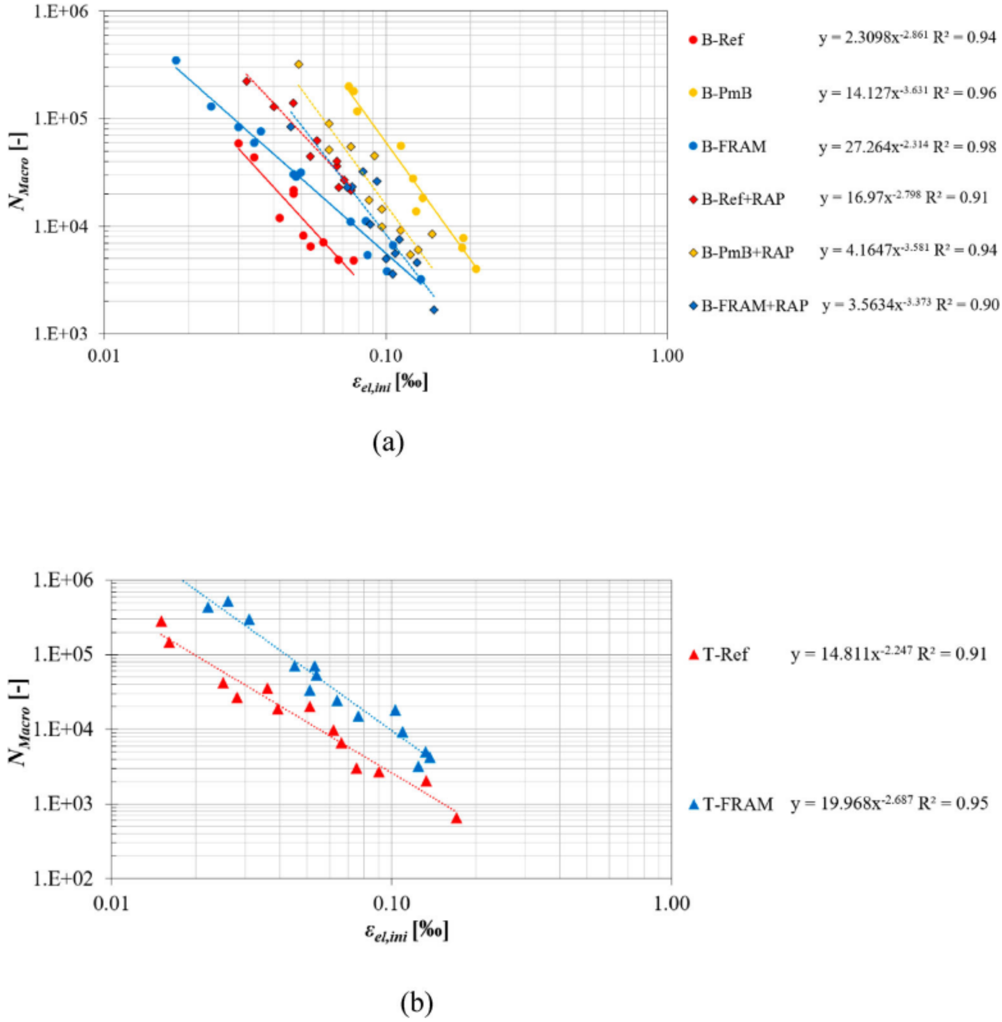

Figure 10. Fatigue results at 20°C: (a) binder layers mixtures with and without RAP; (b) base layers mixtures.

he highlighted that the addition of RAP improves the fatigue resistance at 20°C for the reference and fibre reinforced asphalt mixtures, while significantly reduce the fatigue performances of the PmB mixture. For the base layer mixtures, the fatigue line of the *T-FRAM* is significantly higher than the one of *T-Ref*, indicating a better fatigue resistance for the mixture containing fibres.

In Table 7, the values of ε_6, which is the strain value at 10^6 cycles, for all the mixtures are reported. A higher value of ε_6 implies a higher resistance to fatigue failure. Comparing the values reported in Table 7, the polymer modified mixtures (*B-PmB* and *B-PmB + RAP*) always show the best fatigue performance, followed by the fibre reinforced mixtures (*B-FRAM* and *B-FRAM + RAP*), while *B-Ref* and *B-Ref + RAP* showed the worst fatigue performance. Looking at the parameters of the RAP mixtures, less differences in the ε_6 values can be found. For the base layers' mixtures, ε_6 for *T-FRAM* is more than the double of *T-Ref*.

To further evaluate fatigue performances, in Figures 11(a,b), the initial stiffnesses obtained at the same stress levels for the binder layers mixture without and with RAP are plotted in a bar chart. Figure 11(c) reports similar bar chart for the base layer mixtures. Error bar with standard deviation were also

Table 7. Strain value at 10^6 cycles.

Mixtures	ε_6[‰]	Mixtures	ε_6[‰]	Mixtures	ε_6[‰]
B-Ref	0.009	*B-Ref + RAP*	0.020	*T-Ref*	0.007
B-PmB	0.046	*B-PmB + RAP*	0.031	*T-FRAM*	0.018
B-FRAM	0.011	*B-FRAM + RAP*	0.024		

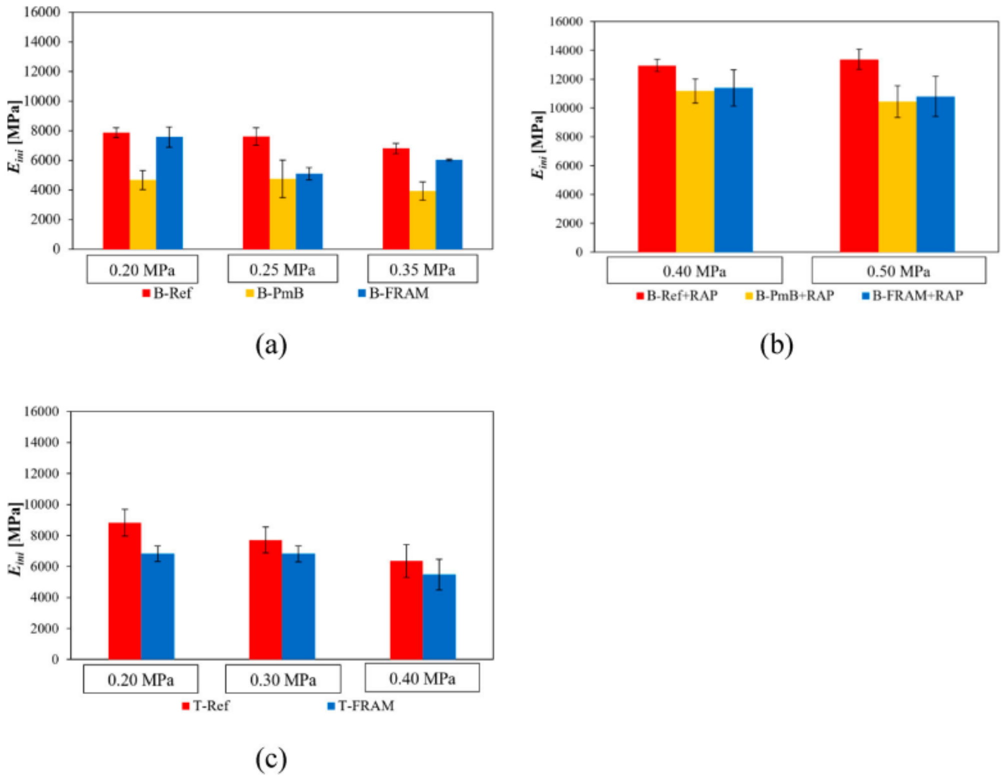

Figure 11. Initial stiffness at the same stress levels: (a) binder layers' mixtures without RAP; (b) binder layers' mixtures containing RAP; (c) base layers' mixtures.

plotted in Figure 11. It was observed that mixtures prepared with plain binder (*B-Ref, B-Ref + RAP, T-Ref*) have higher initial stiffness than the polymer modified ones, and in most cases, also of the fibre reinforced ones (*B-PmB, B-PmB + RAP, B-FRAM, B-FRAM + RAP, T-FRAM*). In some cases, the differences are about 50%. Therefore, the worst fatigue performance of the reference and FRAM mixtures could be also attributed to the higher initial stiffness values observed.

Analyzing all fatigue results, it can be concluded that the addition of fibres could improve fatigue resistance in comparison with the reference mixtures, but they are unable to reach the high quality performance of polymer modified mixtures.

3.5. *Mechanistic pavement design results*

According to Equation 8, the Miner summations for a design period of 30 years were calculated and shown in Table 8. Such results were determined by the strains at the bottom of the asphalt base course and the present traffic load using material specific fatigue functions. According to design conventions, the pavement structure considered does not comply with the design life, since the Miner sum results were higher than the value of 1. However, the addition of fibres lead to a relatively lower Miner sum

Table 8. Miner sums of asphalt variants.

Variants	*T-Ref*	*T-FRAM*
SMA + B-Ref.	5.678	1.446
SMA + B-PmB	6.113	1.574
SMA + B-FRAM	5.754	1.473
SMA + B-Ref + RAP	5.391	1.361
SMA + B-PmB + RAP	5.507	1.396
SMA + B-FRAM + RAP	5.504	1.394

Table 9. TSRST results.

Mixtures	Failure temperature T_F[°C]	SD	Failure stress σ_F[MPa]	SD
B-Ref	−19.1	1.39	3.052	0.26
B-PmB	−29.5	1.39	4.687	0.43
B-FRAM	−21.4	0.83	2.655	0.17
B-Ref + RAP	−16.9	1.34	3.650	0.08
B-PmB + RAP	−23.0	0.82	4.371	0.27
B-FRAM + RAP	−16.2	0.70	3.039	0.36
T-Ref	−22.5	0.67	2.777	0.18
T-FRAM	−17.5	0.53	2.073	0.23

* SD: Standard deviation.

values indicating a longer service life compared to the reference and PmB mixtures. This is especially true for base layer mixtures and mixtures containing high RAP content.

3.6. Thermal cracking tests and thermal fracture results

3.6.1. Thermal stress restrained specimen test (TSRST)

Table 9 summarises the TSRST results reporting the average values of the fracture temperatures (T_F) and of the failure stresses (σ_F) between three replicates for each mixture. The standard deviation is reported to show the repeatability of the tests.

It can be seen that the mixtures containing fibres (*B-FRAM*, *B-FRAM + RAP*) are not able to reach the performance at low temperature of the polymer modified mixtures (*B-PmB*, *B-PmB + RAP*), while presenting similar thermal cracking resistance to the corresponding reference mixtures (*B-Ref*, *B-Ref + RAP*). In particular, comparing *B-FRAM* and *B-FRAM + RAP* with *B-PmB* and *B-PmB + RAP* a difference of about 8 and 7°C in the failure temperatures can be found, while *T-FRAM* and *T-Ref* differs about 5°C. For the base layer mixture, it should be also considered that for *T-FRAM*, a lower penetration grade binder (35/50 instead of 50/70) was used which negatively affects the low temperature performance. Regarding the mixtures containing RAP it can be seen that the failure temperatures are much higher than for the corresponding mixtures without RAP, due to the negative stiffening effect at low temperature of the aged RAP binder incorporated in the mixtures. It can be concluded from the TSRST results that the fibres seem to have no significant effects on low temperature performance of the mixtures with and without RAP.

3.6.2. Semi circular bending test (SCB)

In Table 10, the results of the SCB tests are summarised in terms of nominal stress, σ_{max}, fracture toughness, K_{IC}, and fracture energy, G_F, for all the mixtures. Standard deviations are also listed for each parameter and for each mixture. Good repeatability (most of the standard deviations are less than 10%) was observed for all the mixtures, this is consistent with previous work (Nsengiyumva et al., 2017).

It can be seen that for the binder layers' materials, the polymer modified mixtures (*B-PmB*, *B-PmB + RAP*) showed the highest σ_{max} and K_{IC}, while the fibre reinforced mixtures (*B-FRAM*, *B-FRAM + RAP*) presented the lowest values. Moreover, it can be noted that the differences between

Table 10. SCB results.

Mixtures	σ_{max}[MPa]	SD	K_{IC} [MPa*m$^{0.5}$]	SD	G_F [J/m^2]	SD
B-Ref.	0.798	0.073	5.943	0.544	0.423	0.067
B-PmB	0.929	0.033	6.787	0.202	0.871	0.196
B-FRAM	0.628	0.069	4.733	0.520	0.514	0.214
B-Ref + RAP	0.898	0.066	6.561	0.479	0.477	0.104
B-PmB + RAP	0.970	0.031	7.242	0.213	0.557	0.023
B-FRAM + RAP	0.831	0.119	6.169	0.978	0.585	0.015
T-Ref.	0.655	0.040	4.895	0.284	0.430	0.068
T-FRAM	0.660	0.073	4.834	0.529	0.391	0.055

* SD: Standard deviation.

these parameters were larger for the mixtures composed with fresh materials, while the difference vanished when RAP was used. In addition, an overall increment of σ_{max} and K_{IC} was found when RAP was added, this is especially true for *B-FRAM + RAP*. This indicates a better thermal loading resistance before a macro crack occurs. In the case of fracture energy, G_F, both reference mixtures (*B-Ref*, *B-Ref + RAP*) showed the lowest value among all the six mixtures, while *B-PmB* and *B-FRAM + RAP* present the highest values. Hence, it has to be highlighted that for the polymer modified mixtures, the addition of RAP (*B-PmB + RAP*) decreased G_F, while similar values were found for the other two mixtures (*B-Ref + RAP*, *B-FRAM + RAP*). The differences of G_F between mixtures containing RAP are smaller compared to fresh materials. Moreover, the addition of fibres makes the mixture softer and more elastic which is ultimately leading to a higher G_F. Therefore, it can be concluded that the use of fibres can improve fracture energy in comparison to the reference mixture, but it is not able to achieve similar properties to the polymer modified mixtures when fresh materials are used. Looking at the results of RAP mixtures, it can be seen that the addition of RAP improved the thermal fracture properties of reference and FRAM mixtures, but led to worse fracture performance for PmB mixture. For the base layer mixtures (*T-Ref and T-FRAM*), no remarkable differences were found in all the three parameters indicating that the addition of fibres to a mixture composed with a harder binder (35/50) can lead to similar thermal fracture resistance to the one of the reference mixture composed with a traditional 50/70 binder.

It can be concluded that the addition of fibres can improve the low temperature fracture resistance of the asphalt mixture compared to the reference mixture after the macro crack occurs, this is especially true when RAP is added. In addition, FRAM mixtures containing RAP (*B-FRAM + RAP*) could also reach similar properties of mixtures containing PmB binders (*B-PmB + RAP*). The use of fibres in base layer could soften the hard binder that could ultimately reach similar thermal fracture resistance to the one of 50/70 binder.

4. Summary and conclusions

In this present work, the effects of the addition of polyacronitrile (PAN) fibres on the mechanical properties at high, intermediate and low temperatures of asphalt mixtures for binder and base layers with and without RAP were investigated. In particular, water sensitivity tests were performed to evaluate the moisture resistance, tension-compression tests over a wide range of temperatures and frequencies were carried out to measure the stiffness moduli and the phase angles in the linear viscoelastic range (LVE). Hamburg Wheel Tracking (HWT) tests were conducted at high temperature to determine the resistance to permanent deformation. Indirect Tensile Tests were performed at intermediate temperature to evaluate fatigue resistance, while for evaluation of low temperature performance, Thermal Stress Restrained Specimen (TSRST), and Semi-Circular Bending (SCB) tests were carried out. From the experimental analysis and modelling the following conclusions can be drawn:

- The addition of the fibres significantly worsens the moisture resistance of the mixtures. Therefore, Fibre Reinforced Asphalt Mixtures (FRAM) need more binder to work properly in both dry and wet conditions.

- For stiffness response, the addition of the fibres seems to make the mixtures softer and more elastic at low temperature, lower complex moduli and phase angle were found in FRAM compared to the reference ones. At high temperature, a higher E_0 in FRAM mixtures indicate that fibre acts as a reinforcement.
- The addition of fibres to fresh materials seems to have limited effect on binder rheology as shown from the parameters k, h, α and β of the 2S2P1D model, but it has remarkable effects on the characteristic time τ_0, in fact, the mixture containing fibres present a shorter relaxation time.
- Similar trends in the Cole–Cole and black diagrams were found for the mixture with and without RAP. Both FRAM mixtures present the lowest value of the loss moduli and phase angle in comparison with the reference and PmB mixtures.
- A high content of RAP makes the material more stiffer. According to the 2S2P1D model parameters, the binders' rheological behaviour changeed significantly. In fact, the parameters k and h increase, while α decreases significantly passing from the fresh mixtures to the RAP ones.
- FRAM mixtures achieved better permanent deformation and fatigue resistance to of the compared to the reference mixtures. Slightly weaker anti rutting performance and remarkable reduction in fatigue performance were observed compared to the PmB mixtures. According to the German mechanistic pavement design, the use of fibre leads to better service life, this is especially true when the fibre was used in the base layer.
- The addition of fibres seems to have only limited effect on low temperature cracking resistance and fracture cracking resistance properties before the initial low temperature cracking occurs in mixtures with and without RAP. However, remarkable improvements in the crack propagation resistance properties were found in FRAM, especially in FRAM prepared with RAP.

The overall results of the present research efforts confirm that the addition of fibres can improve fatigue and rutting resistance without compromising the thermal cracking resistance. This is true for both binder and base layers' mixtures with and without RAP. However, this is not sufficient to reach the properties of high quality polymer modified mixtures. Therefore, FRAM mixtures are recommended to be used in areas or regions characterised by mild and high temperatures, while for their use in cold and humidity regions more studies are needed to safely use them. In particular, an optimum mix design with higher content of binder for FRAM mixture is under investigation, since fibers should be properly covered by the bitumen to ensure an adequate mixture behaviour in wet conditions; and also an optimisation of the fibre dosage will be further evaluated to improve the overall mechanical performances.

Disclosure statement

No potential conflict of interest was reported by the author(s).

Funding

This work was supported by Conference of European Directors of Roads (CEDR) [Grant Number 867481].

ORCID

Chiara Riccardi http://orcid.org/0000-0003-4828-4850
Di Wang http://orcid.org/0000-0001-9018-0719
Michael P. Wistuba http://orcid.org/0000-0002-4406-7050

References

Asib, A. S. M., Romero, P., & Safazadeh, F. (2019). An equivalence between methods of aging for determining the low-temperature performance of hot-mix asphalt concrete mixtures containing reclaimed asphalt pavement. *Construction and Building Materials*, *223*, 198–209. https://doi.org/10.1016/j.conbuildmat.2019.06.204

Aurangzeb, Q., Al-Qadi, I. L., Ozer, H., & Yang, R. (2014). Hybrid life cycle assessment for asphalt mixtures with high RAP content. *Resources, Conservation and Recycling*, *83*, 77–86. https://doi.org/10.1016/j.resconrec.2013.12.004

Bueno, M., & Poulikakos, L. D. (2020). Chemo-mechanical evaluation of asphalt mixtures reinforced with synthetic fibers. *Frontiers in Built Environment*, *6*, 41, 1–9. https://doi.org/10.3389/fbuil.2020.00041

Button, J. W., & Hunter, T. G. (1984). *Synthetic fibers in asphalt paving mixtures*. Texas Transportation Institute, Texas A&M University System College Station.

Cannone Falchetto, A., Moon, K. H., Wang, D., Riccardi, C., & Wistuba, M. P. (2018). Comparison of low-temperature fracture and strength properties of asphalt mixture obtained from IDT and SCB under different testing configurations. *Road Materials and Pavement Design*, *19*(3), 591–604. https://doi.org/10.1080/14680629.2018.1418722

Chen, H., & Xu, Q. (2010). Experimental study of fibers in stabilizing and reinforcing asphalt binder. *Fuel*, *89*(7), 1616–1622. https://doi.org/10.1016/j.fuel.2009.08.020

Chen, H., Xu, Q., Chen, S., & Zhang, Z. (2009). Evaluation and design of fiber-reinforced asphalt mixtures. *Materials & Design*, *30*(7), 2595–2603. https://doi.org/10.1016/j.matdes.2008.09.030

Di Benedetto, H., Olard, F., Sauzéat, C., & Delaporte, B. (2004). Linear viscoelastic behavior of bituminous materials: From binders to mixes. *Road Materials and Pavement Design*, *5*(sup1), 163–202. https://doi.org/10.1080/14680629.2004.9689992

EN 12591. (2015). *Binder and bituminous binders. Specifications for paving grade binders*. European Committee for Standardization.

EN 12697-12. (2018). *Bituminous mixtures. Test methods. Determination of the water sensitivity of bituminous specimens*. European Committee for Standardization.

EN 12697-2. (2013). *Bituminous mixtures. Test methods. Determination of particle size distribution*. European Committee for Standardization.

EN 12697-22. (2020). *Bituminous mixtures. Test methods. Wheel tracking*. European Committee for Standardization.

EN 12697-23. (2017). *Bituminous mixtures. Test methods. Determination of the indirect tensile strength of bituminous specimens*. European Committee for Standardization.

EN 12697-24. (2018). *Bituminous mixtures. Test methods. Resistance to fatigue*. European Committee for Standardization.

EN 12697-26. (2012). *Bituminous mixtures. Test methods for hot mix asphalt. Stiffness*. European Committee for Standardization.

EN 12697-3. (2013). *Bituminous mixtures. Test methods. Binder recovery: Rotary evaporator*. European Committee for Standardization.

EN 12697-44. (2019). *Bituminous mixtures. Test methods. Crack propagation by semi-circular bending test*. European Committee for Standardization.

EN 12697-46. (2012). *Bituminous mixtures. Test methods. Test methods for hot mix asphalt, Low temperature cracking and properties by uniaxial tension tests*. European Committee for Standardization.

EN 12697-5. (2019). *Bituminous mixtures. Test methods. Determination of the maximum density*. European Committee for Standardization.

EN 13108-8. (2020). *Tracked changes. Bituminous mixtures. Material specifications. Reclaimed asphalt*. European Committee for Standardization.

EN 14023. (2010). *Binder and bituminous binders. Specification framework for polymer modified binders*. European Committee for Standardization.

Eskandarsefat, S., Dondi, G., & Sangiorgi, C. (2019). Recycled and rubberized SMA modified mixtures: A comparison between polymer modified binder and modified fibres. *Construction and Building Materials*, *202*, 681–691. https://doi.org/10.1016/j.conbuildmat.2019.01.045

European Asphalt Pavement Association (EAPA). (2022). *Asphalt in Figures 2020*. Retrieved July 25, 2022, from https://eapa.org/asphalt-in-figures/

Fakhri, M., & Hosseini, S. A. (2017). Laboratory evaluation of rutting and moisture damage resistance of glass fiber modified warm mix asphalt incorporating high RAP proportion. *Construction and Building Materials*, *134*, 626–640. https://doi.org/10.1016/j.conbuildmat.2016.12.168

García, A., Norambuena-Contreras, J., Bueno, M., & Partl, M. N. (2015). Single and multiple healing of porous and dense asphalt concrete. *Journal of Intelligent Material Systems and Structures*, *26*(4), 425–433. https://doi.org/10.1177/1045389X14529029

Gupta, A., Lastra-Gonzalez, P., Castro-Fresno, D., & Rodriguez-Hernandez, J. (2021). Laboratory characterization of porous asphalt mixtures with aramid fibers. *Materials*, *14*(8), 1935, 1–14. https://doi.org/10.3390/ma14081935

Ho, C. H., Shan, J., Wang, F., Chen, Y., & Almonnieay, A. (2016). Performance of fiber-reinforced polymer-modified asphalt: Two-year review in Northern Arizona. *Transportation Research Record*, *2575*(1), 138–149. https://doi.org/10.3141/2575-15

Hugener, M., Wang, D., Cannone Falchetto, A., Porot, L., Kara De Maeijer, P., Orešković, M., Sa-da-Costa, Margarida, Tabatabaee, Hassan, Bocci, Edoardo, Kawakami, Atsushi, Hofko, Bernhard, Grilli, Andrea, Pasquini, Emiliano, Pasetto, Marco, Zhai, Huachun, Soenen, Hilde, Van den bergh, Wim, Cardone, Fabrizio, Carter, Alan, Vasconcelos, Kamilla, Carbonneau, Xavier, Lorserie, Aurelie, Mladenović, Goran, Koudelka, Tomas, Coufalik, Pavel, Zhang, Runhua, Dave, Eshan, Tebaldi, G. (2022). Recommendation of RILEM TC 264 RAP on the evaluation of asphalt recycling agents for hot mix asphalt. *Materials and Structures*, *55*(2), 1–9. https://doi.org/10.1617/s11527-021-01837-0

Kim, M. J., Kim, S., Yoo, D. Y., & Shin, H. O. (2018). Enhancing mechanical properties of asphalt concrete using synthetic fibers. *Construction and Building Materials*, *178*, 233–243. https://doi.org/10.1016/j.conbuildmat.2018.05.070

Klinsky, L. M. G., Kaloush, K. E., Faria, V. C., & Bardini, V. S. S. (2018). Performance characteristics of fiber modified hot mix asphalt. *Construction and Building Materials*, *176*, 747–752. https://doi.org/10.1016/j.conbuildmat.2018.04.221

Landi, D., Marconi, M., Bocci, E., & Germani, M. (2020). Comparative life cycle assessment of standard, cellulose-reinforced and end of life tires fiber-reinforced hot mix asphalt mixtures. *Journal of Cleaner Production*, *248*, Article 119295. https://doi.org/10.1016/j.jclepro.2019.119295

Leiva-Padilla, P., Moreno-Navarro, F., Iglesias-Salto, G., & Rubio-Gámez, M. C. (2019). Analysis of the mechanical response of asphalt materials manufactured with metallic fibres under the effect of magnetic fields. *Smart Materials and Structures*, *29*(1), Article 015033. https://doi.org/10.1088/1361-665X/ab5762

Li, Z., Shen, A., Wang, H., Guo, Y., & Wu, H. (2020). Effect of basalt fiber on the low-temperature performance of an asphalt mixture in a heavily frozen area. *Construction and Building Materials*, *253*, Article 119080. https://doi.org/10.1016/j.conbuildmat.2020.119080

Liu, Y., Su, P., Li, M., You, Z., & Zhao, M. (2020). Review on evolution and evaluation of asphalt pavement structures and materials. *Journal of Traffic and Transportation Engineering (English Edition)*, *7*(5), 573–599. https://doi.org/10.1016/j.jtte.2020.05.003

Majidifard, H., Tabatabaee, N., & Buttlar, W. (2019). Investigating short-term and long-term binder performance of high-RAP mixtures containing waste cooking oil. *Journal of Traffic and Transportation Engineering (English Edition)*, *6*(4), 396–406. https://doi.org/10.1016/j.jtte.2018.11.002

Miner, M. A. (1945). Cumulative damage in fatigue. *Journal of Applied Mechanics*, *12*(3), A159–A164. https://doi.org/10.1115/1.4009458

Monismith, C. L. (2004). Evolution of long-lasting asphalt pavement design methodology: a perspective. *Lecture presented in June 2004 at Auburn University to the ISAP-sponsored International Symposium on Design and Construction of Long Lasting Asphalt Pavements*.

Montañez, J., Caro, S., Carrizosa, D., Calvo, A., & Sanchez, X. (2020). Variability of the mechanical properties of reclaimed asphalt pavement (RAP) obtained from different sources. *Construction and Building Materials*, *230*, Article 116968. https://doi.org/10.1016/j.conbuildmat.2019.116968

Motlagh, A. A., & Mirzaei, E. (2016). Effect of using fibre on the durability of asphalt pavement. *Civil Engineering Journal*, *2*(2), 63–72. https://doi.org/10.28991/cej-2016-00000013

Mukhammadiyeva, G. F., Karimova, L. K., Beigul, N. A., Bakirov, A. B., Valeeva, E. T., Mavrina, L. N., … & Gimaeva, Z. F. (2016). Peculiarities of air pollution in the production of continuous glass fiber. *Gigiena I Sanitariia*, 95(6), 548–551. [In Russia].

Nguyen, M. L., Balay, J. M., Di Benedetto, H., Sauzeat, C., Bilodeau, K., Olard, F., Héritier, B., Dumont, H., Bonneau, D. (2017). Evaluation of pavement materials containing RAP aggregates and hydraulic binder for heavy traffic pavement. *Road Materials and Pavement Design*, *18*(2), 264–280. https://doi.org/10.1080/14680629.2016.1213483

Nguyen, Q. T., Di Benedetto, H., & Sauzéat, C. (2015). Linear and nonlinear viscoelastic behavior of bituminous mixtures. *Materials and Structures*, *48*(7), 2339–2351. https://doi.org/10.1617/s11527-014-0316-5

Nguyen, T., Nguyen, H. T., Tran, D. L., & Nguyen, V. T., & L, M. (2022). Finite element implementation of Huet-Sayegh and 2S2P1D models for analysis of asphalt pavement structures in time domain. *Road Materials and Pavement Design*, *23*(1), 22–46. https://doi.org/10.1080/14680629.2020.1809501

Nsengiyumva, G., You, T., & Kim, Y. R. (2017). Experimental-statistical investigation of testing variables of a semicircular bending (SCB) fracture test repeatability for bituminous mixtures. *Journal of Testing and Evaluation*, *45*(5), 1691–1701. https://doi.org/10.1520/JTE20160103

Office, J. E., Chen, J., Dan, H., Ding, Y., Gao, Y., Guo, M., Guo, Shuaicheng, Han, Bingye, Hong, Bin, Hou, Yue, Hu, Chichun, Hu, Jing, Huyan, Ju, Jiang, Jiwang, Jiang, Wei, Li, Cheng, Liu, Pengfei, Liu, Yu, Liu, Zhuangzhuang, Lu, Guoyang, Ouyang, Jian, Qu, Xin, Ren, Dongya, Wang, Chao, Wang, Chaohui, Wang, Dawei, Wang, Di, Wang, Hainian, Wang, Haopeng, Xiao, Yue, Xing, Chao, Xu, Huining, Yan, Yu, Yang, Xu, You, Lingyun, You, Zhanping, Yu, Bin, Yu, Huayang, Yu, Huanan, Zhang, Henglong, Zhang, Jizhe, Zhou, Changhong, Zhou, Changjun, Zhu, X. (2021). New innovations in pavement materials and engineering: A review on pavement engineering research 2021. *Journal of Traffic and Transportation Engineering (English Edition)*, *8*(6), 815–999. https://doi.org/10.1016/j.jtte.2021.10.001

Olard, F., & Di Benedetto, H. (2003). General "2S2P1D" model and relation between the linear viscoelastic behaviors of bituminous binders and mixes. *Road Materials and Pavement Design*, *4*(2), 185–224. https://doi.org/10.1080/14680629.2003.9689946

Park, K. S., Shoukat, T., Yoo, P. J., & Lee, S. H. (2020). Strengthening of hybrid glass fiber reinforced recycled hot-mix asphalt mixtures. *Construction and Building Materials*, *258*, Article 118947. https://doi.org/10.1016/j.conbuildmat.2020.118947

Pedraza, A., Di Benedetto, H., Sauzéat, C., & Pouget, S. (2021). Properties at low temperatures of asphalt mixes containing high content of multi-recycled RAP. *Journal of Testing and Evaluation*, *50*(2), 1–12. https://doi.org/10.1520/JTE20210209

Possebon, ÉP, Specht, L. P., Di Benedetto, H., Schuster, S. L., & Pereira, D. D. S. (2021). Rheological properties, 2S2P1D modelling and SHStS transformation of 12 Brazilian bitumens and mixtures. *Road Materials and Pavement Design*, 1–18. doi:10.1080/14680629.2021.2010589

Riccardi, C. (2017). *Mechanistic modeling of bituminous mortars to predict performance of asphalt mixtures containing RAP*. Technische Universität Braunschweig. Braunschweig, Germany. ISBN: 978-3-932164-32-3.

Riccardi, C., Cannone Falchetto, A., Losa, M., & Leandri, P. (2017a). Estimation of the SHStS transformation parameter based on volumetric composition. *Construction and Building Materials*, *157*, 244–252. https://doi.org/10.1016/j.conbuildmat.2017.09.083

Riccardi, C., Cannone Falchetto, A., & Wang, D. (2021). Three-dimensional characterization of asphalt mixture containing recycled asphalt pavement. *Journal of Association of Asphalt Paving Technologies*, *2021*(89), 75–94.

Riccardi, C., Cannone Falchetto, A., Wang, D., & Wistuba, M. P. (2017b). Effect of cooling medium on low-temperature properties of asphalt binder. *Road Materials and Pavement Design*, *18*(sup4), 234–255. https://doi.org/10.1080/14680629.2017.1389072

Roberts, F. L., Kandhal, P. S., Brown, E. R., Lee, D. Y., & Kennedy, T. W. (1991). *Hot mix asphalt materials, mixture design and construction*. National Asphalt Pavement Association Education Foundation, First Edition.

Saal, R., & Pell, P. (1960). Fatigue of bituminous mixes. *Kolloid-Zeitschrift Band*, *171*(1/1990), 61–71. https://doi.org/10.1007/BF01520326

Slebi-Acevedo, C. J., Lastra-González, P., Pascual-Muñoz, P., & Castro-Fresno, D. (2019). Mechanical performance of fibers in hot mix asphalt: A review. *Construction and Building Materials*, *200*, 756–769. https://doi.org/10.1016/j.conbuildmat.2018.12.171

Slebi-Acevedo, C. J., Pascual-Muñoz, P., Lastra-González, P., & Castro-Fresno, D. (2021). A multi-criteria decision-making analysis for the selection of fibres aimed at reinforcing asphalt concrete mixtures. *International Journal of Pavement Engineering*, *22*(6), 763–779. https://doi.org/10.1080/10298436.2019.1645848

Smirnova, O., Kharitonov, A., & Belentsov, Y. (2019). Influence of polyolefin fibers on the strength and deformability properties of road pavement concrete. *Journal of Traffic and Transportation Engineering (English Edition)*, *6*(4), 407–417. https://doi.org/10.1016/j.jtte.2017.12.004

Stempihar, J. J., Souliman, M. I., & Kaloush, K. E. (2012). Fiber-reinforced asphalt concrete as sustainable paving material for airfields. *Transportation Research Record*, *2266*(1), 60–68. https://doi.org/10.3141/2266-07

Tasdemir, Y., & Agar, E. (2007). Investigation of the low temperature performances of polymer and fiber modified asphalt mixtures. *Indian Journal of Engineering and Materials Sciences*, *14*(2), 151–157.

Van Winkle, C., Mokhtari, A., Lee, H. D., Williams, R. C., & Schram, S. (2017). Laboratory and field evaluation of HMA with high contents of recycled asphalt pavement. *Journal of Materials in Civil Engineering*, *29*(2), Article 04016196. https://doi.org/10.1061/(ASCE)MT.1943-5533.0001720

Walther, A., & Wistuba, M. (2012). Mechanistic pavement design considering bottom-up and top-down-cracking. In *7th RILEM International Conference on Cracking in Pavements*. 963–973. Delft. Springer, Dordrecht.

Wang, H., Yang, Z., Zhan, S., Ding, L., & Jin, K. (2018). Fatigue performance and model of polyacrylonitrile fiber reinforced asphalt mixture. *Applied Sciences*, 8(10), 1818, 1–12. https://doi.org/10.3390/app8101818

Weise, C., & Zeissler, A. (2016). *Effects of fiber reinforcement on the fatigue and rutting performance of asphalt mixes*. In 6th Eurasphalt & Eurobitume Congress, Prague, Czech Republic.

Williams, M. L., Landel, R. F., & Ferry, J. D. (1955). The temperature dependence of relaxation mechanisms in amorphous polymers and other glass-forming liquids. *Journal of the American Chemical Society*, *77*(14), 3701–3707. https://doi.org/10.1021/ja01619a008

Wistuba, M. P. (2016). The German segmented steel roller compaction method–state-of-the-art report. *International Journal of Pavement Engineering*, *17*(1), 81–86. https://doi.org/10.1080/10298436.2014.925555

Wistuba, M. P., & Walther, A. (2013). Consideration of climate change in the mechanistic pavement design. *Road Materials and Pavement Design*, *14*(sup1), 227–241. https://doi.org/10.1080/14680629.2013.774759

Wu, J., Hong, R., & Gu, C. (2018). Influence of fiber type on low-temperature fracture performance of presawed asphalt mixture beams. *Advances in Materials Science and Engineering*, *2018*, 1–7. https://doi.org/10.1155/2018/5087395

Xu, Q., Chen, H., & Prozzi, J. A. (2010). Performance of fiber reinforced asphalt concrete under environmental temperature and water effects. *Construction and Building Materials*, *24*(10), 2003–2010. https://doi.org/10.1016/j.conbuildmat.2010.03.012

Zaumanis, M., & Mallick, R. B. (2015). Review of very high-content reclaimed asphalt use in plant-produced pavements: State of the art. *International Journal of Pavement Engineering*, *16*(1), 39–55. https://doi.org/10.1080/10298436.2014.893331

Zaumanis, M., Mallick, R. B., Poulikakos, L., & Frank, R. (2014). Influence of six rejuvenators on the performance properties of reclaimed asphalt pavement (RAP) binder and 100% recycled asphalt mixtures. *Construction and Building Materials*, *71*, 538–550. https://doi.org/10.1016/j.conbuildmat.2014.08.073

Zhang, C., Ren, Q., Qian, Z., & Wang, X. (2019). Evaluating the effects of high RAP content and rejuvenating agents on fatigue performance of fine aggregate matrix through DMA flexural bending test. *Materials*, *12*(9), 1508, 1–15. https://doi.org/10.3390/ma12091508

Zhong, Y. X., Wang, X. L., & Liao, M. J. (2011). Experiment research on performance of low-temperature crack resistance of reinforced asphalt mixtures. In Lijuan Li (Ed.), *Advanced materials research* (Vol. 163, pp. 1128–1133). Trans Tech Publications Ltd.

Zhou, Z., Gu, X., Jiang, J., Ni, F., & Jiang, Y. (2019). Fatigue cracking performance evaluation of laboratory-produced polymer modified asphalt mixture containing reclaimed asphalt pavement material. *Construction and Building Materials*, *216*, 379–389. https://doi.org/10.1016/j.conbuildmat.2019.05.031

Ziari, H., Aliha, M. R. M., Moniri, A., & Saghafi, Y. (2020). Crack resistance of hot mix asphalt containing different percentages of reclaimed asphalt pavement and glass fiber. *Construction and Building Materials*, *230*, Article 117015. https://doi.org/10.1016/j.conbuildmat.2019.117015